RSC Advances

PAPER

View Article Online
View Journal | View Issue

Cite this: *RSC Adv.*, 2024, **14**, 11533

Formulating compatible non-flammable electrolyte for lithium-ion batteries with ethoxy (pentafluoro) cyclotriphosphazene

Yutao Liu, * Jiazheng Lu, Xuanlin Gong, Jingju Liu, Baohui Chen, Chuanping Wu and Zhen Fang

Lithium (Li) ion batteries have played a great role in modern society as being extensively used in commercial electronic products, electric vehicles, and energy storage systems. However, battery safety issues have gained growing concerns as there might be thermal runaway, fire or even explosion under external abuse. To tackle these safety issues, developing non-flammable electrolytes is a promising strategy. However, the balance between the flame-retarding effect and the electrochemical performance of electrolytes remains a great challenge. Herein, we evaluate the function of ethoxy (pentafluoro) cyclotriphosphazene (**PFPN**) as an effective flame-retarding additive for lithium-ion batteries. The flammability of electrolytes is greatly suppressed with the introduction of a small amount of **PFPN**. Moreover, **PFPN** exhibited excellent compatibility with $LiFePO_4$ (LFP) cathode and graphite (Gr) anode, the electrochemical performances of LFP|Li and Gr|Li half cells are virtually unaffected. Scanning electron microscope (SEM) and X-ray photoelectron spectroscopy (XPS) reveal the stable interphase between **PFPN**-containing electrolyte and LFP and Gr electrodes. Fourier transform infrared spectroscopy (FT-IR), Raman and nuclear magnetic resonance (NMR) spectra demonstrate the introduction of **PFPN** only exhibits negligible influence on the solvation structure of electrolyte. Benefiting from these merits of **PFPN**, the LFP|Gr cell shows desirable long-term cycling performance, which demonstrates great potential for practical application.

Received 19th March 2024
Accepted 4th April 2024

DOI: 10.1039/d4ra02095b

rsc.li/rsc-advances

1. Introduction

Li ion batteries have played a great role in our daily life, such as commercial electronic products, electric vehicles, and energy storage systems. However, the common electrolyte of Li ion batteries is mainly composed of Li salt (typically, $LiPF_6$ is used), carbonate solvents and other additives, and these carbonate solvents could be ignited steadily when a battery thermal runaway happens, which further lead to fire disaster or even explosion.[1–3] To tackle these safety issues, one promising strategy is to develop non-flammable electrolyte, and much progress has been made.

Applying flame retardant additive to formulate non-flammable electrolyte has long been regarded as an ideal routine, as a small amount of additive will not bring great change to the physico-chemical property of electrolyte, while the flammability could be highly suppressed.[4–6] Among the flame-retarding additives, phosphates were the most studied, and a serial of compounds were found to exhibited excellent flame retardant capability, such as trimethyl phosphate (**TMP**),[7,8] triphenyl phosphate (TTP),[9] trimethyl phosphite (**TMPi**),[10] tris(2,2,2-trifluoroethyl) phosphate (TFEP),[11] *etc.* Nevertheless, these phosphate-based additives were found to present poor reduction stability, which leads to severe side reactions when contact with Gr anode.[12–14] Balancing the flame-retarding effect and the electrochemical performance of electrolytes remains a great challenge till now.[15–18]

Herein, ethoxy (pentafluoro) cyclotriphosphazene (**PFPN**) was applied as the flame-retarding additive for Li ion battery electrolyte. The flammability of electrolyte was greatly suppressed with introduction of only 3 wt% **PFPN**. The compatibility of **PFPN**-containing electrolyte was studied in LFP|Li and Gr|Li half cells, both exhibited comparable performance to base electrolyte. SEM and XPS revealed **PFPN** helped to form stable electrode/electrolyte interphase, thus prevent continuous parasitic reactions. FT-IR, Raman and NMR spectra demonstrated the electrolyte solvation structure was not greatly changed with **PFPN** additive. Benefiting from these merits of **PFPN**, LFP|Gr cell presented desirable long-term stability, which demonstrates great potential for practical application.

2. Experimental sections

2.1 Materials

TMP (99.8%), **TEP** (99.8%), **TMPi** (99.8%), **TEPi** (99.8%) and **PFPN** (99.9%) were purchased from DoDo Chem and used as received. 1 M $LiPF_6$ in EC : DMC (v/v = 1 : 1) was purchased from

State Key Laboratory of Disaster Prevention and Reduction for Power Grid Transmission and Distribution Equipment, State Grid Hunan Electric Company Limited Disaster Prevention and Reduction Center, Changsha, Hunan, China. E-mail: ytliu_whu@126.com

Zhangjiagang Guotai Huarong New Chemical Materials Co., Ltd, and used as the base electrolyte.

2.2 Preparation of electrolyte and electrode

All the electrolytes used in experiments were prepared by adding a certain amount of additive to the base electrolyte, and stirred at room temperature for 24 h before use.

Commercial LFP (LF0608) and Gr (SM0205) electrodes were purchased from Canrd Company, the active material ratios were 91.5% and 95.7% respectively. The areal capacity was ~1.58 mA h cm^{-2} (~10.5 mg cm^{-2}) for LFP, and ~1.89 mA h cm^{-2} (~5.55 mg cm^{-2}). All the electrodes were vacuum dried for 12 hours before use.

2.3 Electrochemical measurement

Cycling tests of CR2032 coin cells were conducted on LAND electrochemical testing system (LANHE, China). The LFP|Li and LFP|Gr cells were cycled between 4.0 and 2.5 V, and three formation cycle at 0.1C were conducted for each cell. The Gr|Li cells were cycled between 1.5 and 0.005 V, and three formation cycle at 0.2C were conducted for each cell.

The electrochemical stability of electrolyte was determined by linear sweep voltammetry (LSV) test, where Al foil was used as the working electrode, and Li foil was used as counter electrode and reference electrode. The potential range was set from open-circuit potential (OCP) to 6.0 V (*vs.* Li^+/Li), and the scanning rate was 1 mV s^{-1}.

2.4 Characterization

Morphology was observed on scanning electron microscope (SEM, ZEISS Merlin Compact). Surface species on the anode were determined by X-ray photoelectron spectroscopy (XPS, Thermo scientific ESCALAB250Xi, USA), and monochromatic Al-K_α was used as the X-ray source. The electrodes acquired from cycled cells were thoroughly washed with DMC before transferred to an argon-filled vessel for SEM and XPS characterization. The FT-IR and Raman spectra were conducted with NICOLET 5700 FT-IR Spectrometer and Renishaw InVa Raman spectrometer respectively. The NMR spectra were conducted with BRUKER AVANCE 400.

The self-extinguishing time (SET) test was conducted by adding a certain amount of electrolyte into a dry watch glass and recording the burning time after ignition. The SET was calculated as following:

$$\mathrm{SET} = \frac{t}{m}$$

where t is the burning time, and m is the mass of electrolyte, and each electrolyte was tested for three time to ensure data reliability.

The ionic conductivity of electrolyte was directly tested with DDBJ-350 (Leici Company, China) at room temperature.

3. Results and discussion

3.1 Flame-retarding effect of PFPN

To examine the flame retardant effect of **PFPN**, it was added into the base electrolyte (1 M $LiPF_6$ EC : DMC (v/v = 1 : 1)) for self-extinguishing time (SET) test, and other common flame-retarding additives were also studied for comparison. As is shown in Fig. 1a, the base electrolyte exhibited a SET of 53.4 s g^{-1}, indicating the high flammability of it. When flame-retarding additives were added, the SETs of electrolytes showed distinct drop, and it presented a clear relationship with the content of additive. Nevertheless, the SETs were still as high as ~20 s g^{-1} even with 20 wt% content for the common flame-retarding additives (**TMP**, **TEP**, **TMPi** and **TEPi**), demonstrating the inadequate flame retardancy. According to previous reports,[12,13] higher content of flame-retarding additives would lead to worse electrochemical performance, as the additives usually possessed poor reduction stability. In order to prevent the degradation of cycling performance, it was necessary to develop additive with higher flame-retarding efficiency or better compatibility. In sharp contrast to the common additives, the electrolyte would not be ignited when 5 wt% **PFPN** was added, and the contents to realize a SET lower than 20 s g^{-1} or 10 s g^{-1} were only 1 wt% and 3 wt%. Fig. 1b shows the structures of each additive, and the superior flame retardancy of **PFPN** should be mainly originated from the phosphonitrile structure. According to previous reports,[19–21] the good flame-retardant effect and thermal stability of fluorinated cyclophosphazene come from its high P content and the synergistic effect between P, F, and N, and that the F helps improve the battery's electrochemical performance and overall cycling stability. The flammability comparison of base electrolyte with/without 3 wt% **PFPN** was also provided in Fig. 1c, and it could be seen that the flame was strong and continuous for the base electrolyte, while only part of the 3% **PFPN** electrolyte was ignited for a short time. Apart from lowering the extinguishing time, the released heat was also much lower, which would greatly decrease the possibility of safety hazard.

3.2 Electrochemical performance of PFPN-containing electrolyte

In addition to the flame retardancy, the influences on other electrolyte properties were also important for developing an ideal flame-retarding additive. The ionic conductivity of electrolyte with various flame-retarding additives was first evaluated, and the result is shown in Fig. 2a. In terms of the overall trend, all the ionic conductivities decreased as more additives were used. It was surprising to find that **PFPN** not only possessed highly flame-retarding efficiency, it also exhibited little effect on ionic conductivity. In details, the ionic conductivity could maintain >9 mS cm^{-1} with a SET of 0–20 s g^{-1}, which is already sufficient for most application scenarios. Considering both the flame retardancy and ionic conductivity, 3 wt% **PFPN**-containing electrolyte was selected as the optimized recipe, and its electrochemical stability was also examined. As is shown in Fig. 2b, the 3% **PFPN** electrolyte showed a small peak around 4.2 V, which should be ascribe to the oxidation of **PFPN**. Nevertheless, the introduction of **PFPN** will not greatly affect the stability of cathode-electrolyte interphase, and this would be confirmed later in the cycling test and XPS characterization.

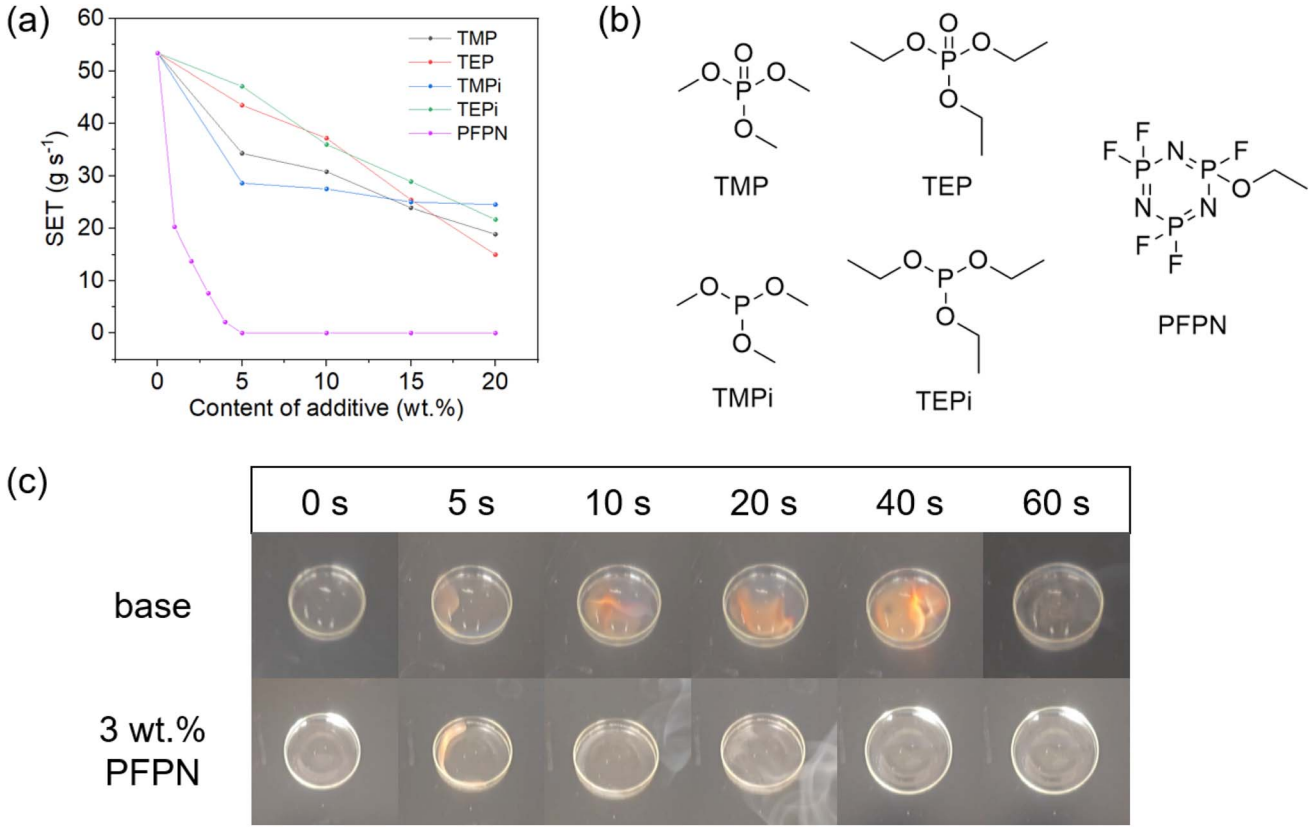

Fig. 1 (a) SET of electrolytes with different flame-retarding additives. (b) Structures of different flame-retarding additive. (c) Flammability of base electrolyte with/without 3 wt% **PFPN**.

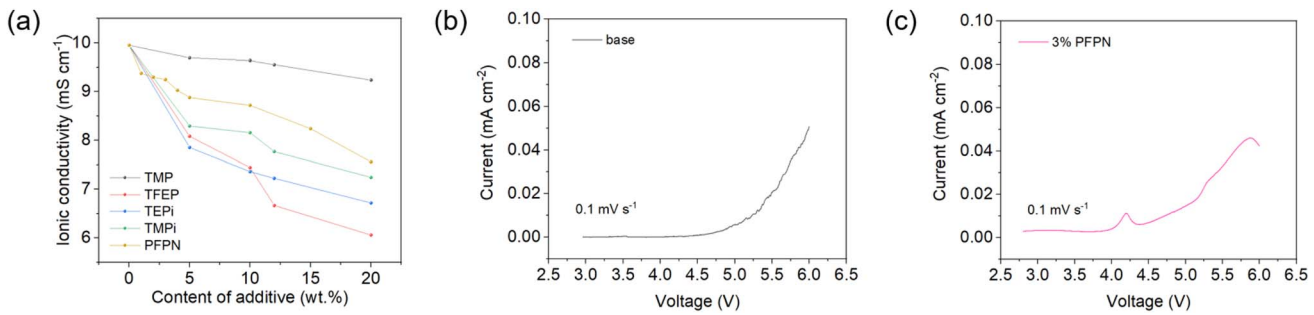

Fig. 2 (a) Ionic conductivities of electrolytes with various flame-retarding additives. (b and c) Electrochemical stability of base and 3% **PFPN** electrolyte.

LFP|Li and Gr|Li half cells were assembled for the evaluation of electrochemical performance of 3% **PFPN** electrolyte, and the result was shown in Fig. 3. As is shown in Fig. 3a, the cycling performance of LFP|Li cell with 3% **PFPN** electrolyte was quite similar to the cell with base electrolyte. Both cells exhibited stable discharge capacity, and negligible deterioration was observed even after 100 cycles. Therefore, **PFPN** should possess good compatibility with LFP cathode, and this confirmed the oxidation of **PFPN** (Fig. 2c) would not be a great issue. Fig. 3b shows the evolution of polarization during cycling, and the stable curves fully demonstrated the stability of cathode–electrolyte interphase.

The stability of anode–electrolyte interphase is also of great importance, as most flame-retarding additives were found to form unstable solid electrolyte interphase (SEI), which further lead to degradation of cycling performance and thus hinder the practical application. Fig. 3c shows the electrochemical performance of Gr|Li cell with base and 3% **PFPN** electrolyte, and it could be seen that the addition of **PFPN** would lead to slightly lower capacity during the first few cycles. However, the capacity became stable after the initial period, and little difference was observed during the following cycles. This phenomenon suggested that **PFPN** might be reduced in the initial cycles, but a stable SEI could be formed and prevent

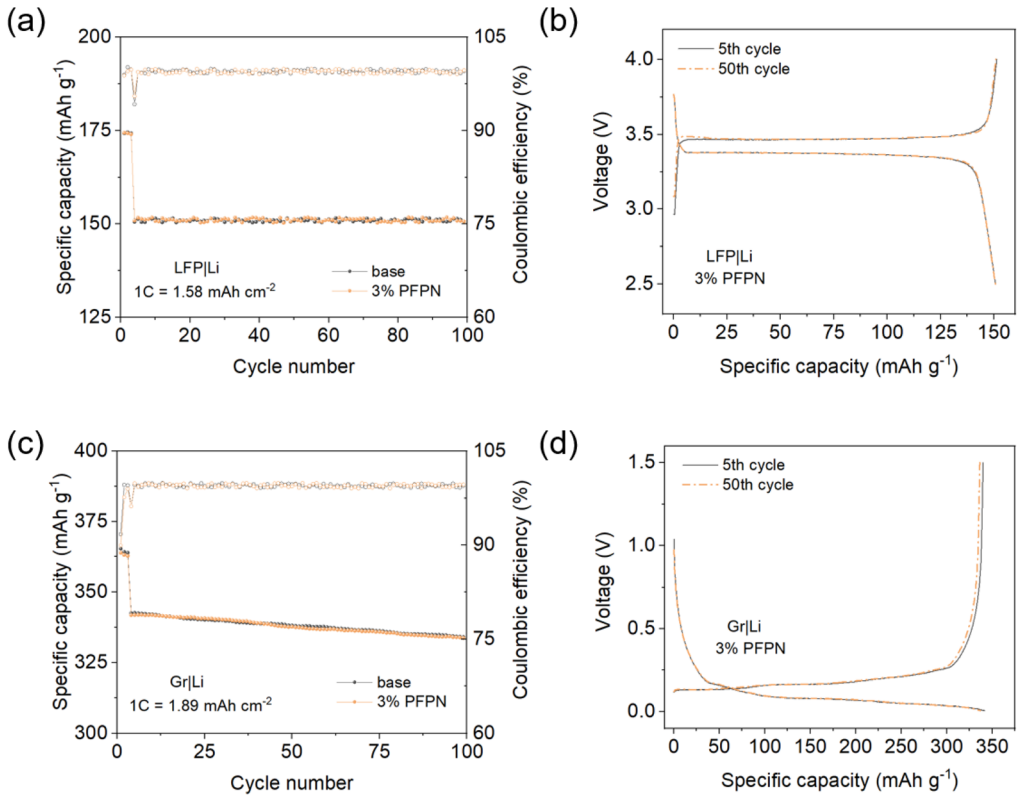

Fig. 3 (a and c) Cycling performances of LFP|Li and Gr|Li cells with different electrolytes. (b and d) Voltage profiles of LFP|Li and Gr|Li cell with 3% PFPN electrolyte.

continuous side reactions. This assumption was further supported by the voltage profiles of Gr|Li cell (Fig. 3d), where the polarization curves did not change greatly from 5th to 50th cycle.

3.3 Interphase characterization of PFPN-containing electrolyte

Considering the desirable electrochemical performance and electrode compatibility, it is necessary to explore the underlying mechanism. To achieve this target, LFP and Gr electrodes after 50 cycles in base and 3% **PFPN** electrolyte were acquired from the corresponding half cells, and wash thoroughly with DMC to remove the residual electrolyte. After that, the electrodes were vacuum dried and transferred in Ar-filled container for SEM and XPS tests. According to previous reports,[22–24] the morphology of cathode/anode interface would be greatly changed if there were severe side reactions of electrolyte. However, Fig. 4 showed that the morphology of LFP electrode before and after cycling did not change greatly. Additionally, Gr electrodes cycled in base or 3% **PFPN** electrolyte were also quite similar, thus the anode–electrolyte interphase should not be evidently affected by the **PFPN**. Nevertheless, it is still necessary to study the compatibility with other characterizations.

Besides the morphology of electrode, understanding the composition evolution of electrode–electrolyte interphase is also of great importance, thus the LFP and Gr electrodes after 50 cycles were examined by XPS test. As is shown in Fig. 5a, there was no great change with the introduction of 3 wt% **PFPN**, except the signal of LFP was slightly decreased, suggesting the thickness of CEI might be higher.[2] The N 1s spectra (Fig. 5b) also showed similar trend, as LiN_xO_y was detected for 3% **PFPN** group.[25] Nevertheless, the composition of CEI was generally stable as is depicted in Fig. 5c, and this should contribute to the good compatibility between 3% **PFPN** electrolyte and LFP cathode. The influence on SEI structure was also examined, and some interesting results were found. As is shown is Fig. 5d, there was weak signal of LiP_xF_y and $LiP_xO_yF_z$ for base group, which should be derived from the decomposition of PF_6^-. However, these signals disappeared when **PFPN** was added. Fig. 5e exhibited there were N-containing species (LiN_xO_y and Li_3N) formed, both were reported to enhance the stability of SEI.[26,27] Overall, these changes of SEI were also reflected in Fig. 5f, and it was evident to see there were more N and less P content. Considering the harmful effect of traditional flame-retardant additive was originated from the P-containing species, this specific N-rich SEI should contribute to the superior compatibility of 3% **PFPN** electrolyte and Gr anode.

Based on the above characterization and analysis, it could be concluded that 3% **PFPN** electrolyte exhibited excellent flame-retarding efficiency and desirable compatibility toward LFP and Gr electrodes. Consequently, the solvation structure of **PFPN**-containing electrolyte was studied to better understand the excellent performance. As is shown in Fig. 6a and b, the coordination of state of EC and DMC were studied by FT-IR

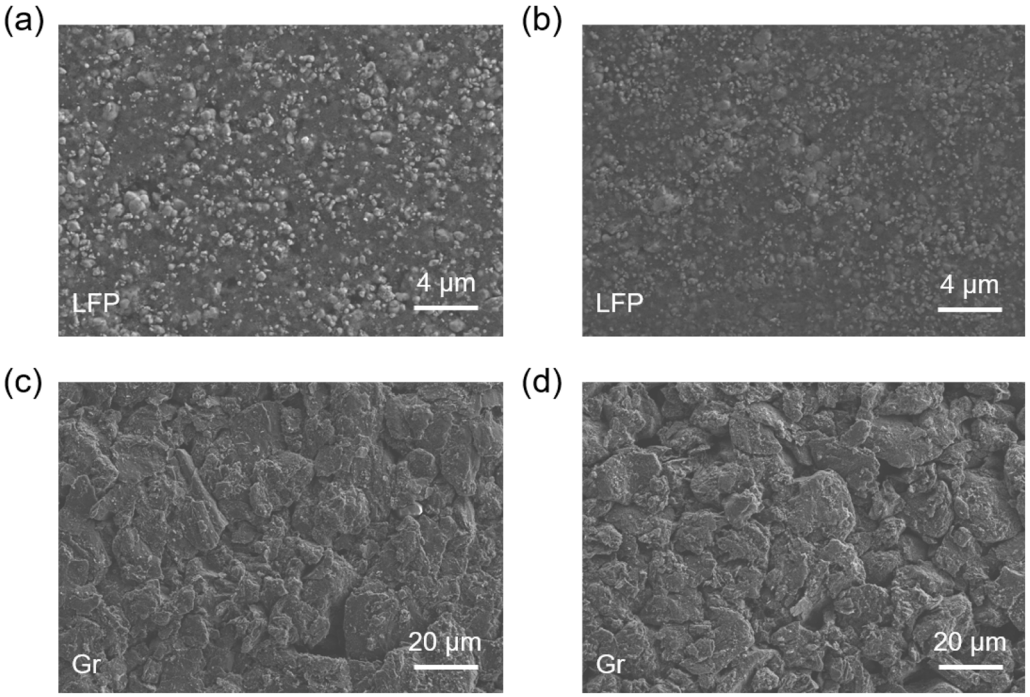

Fig. 4 SEM images of LFP and Gr electrodes cycled 50 times (a and c) base electrolyte and (b and d) 3% **PFPN** electrolyte.

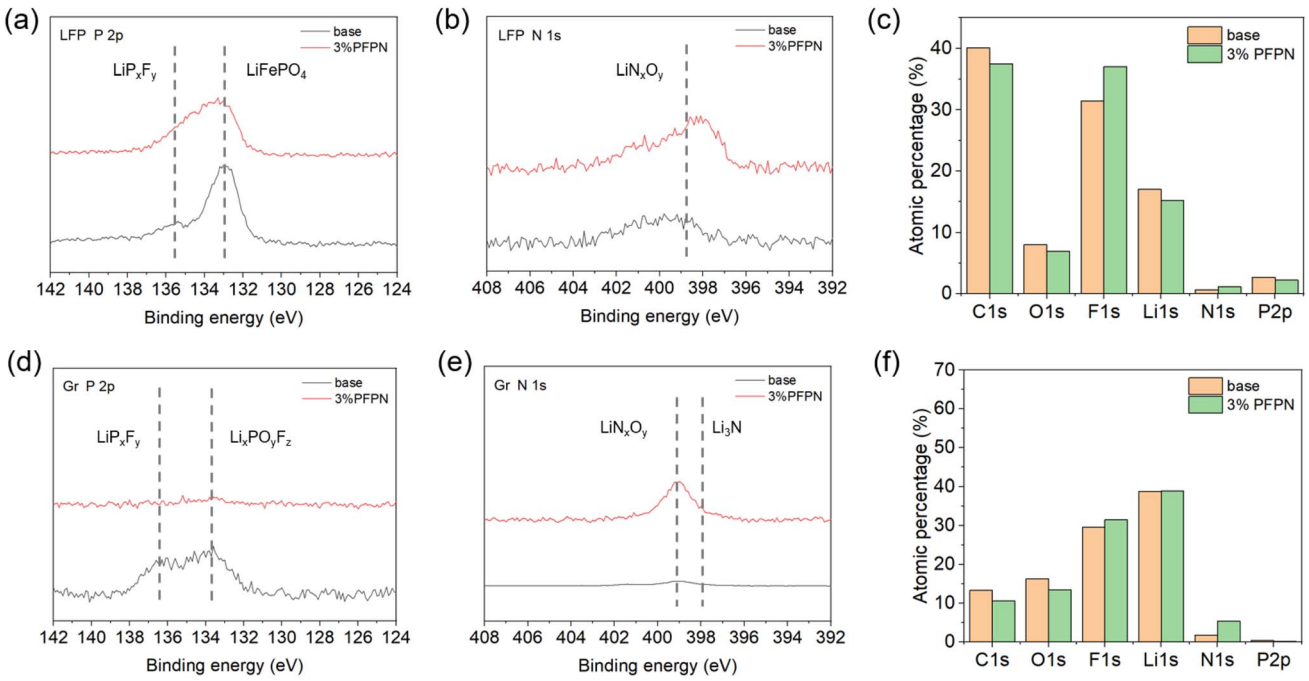

Fig. 5 XPS profile of LFP and Gr electrodes after 50 cycles (a and d) P 2p, (b and e) N 1s spectra and (c and f) atomic percentage profile.

spectra, and the main signals were labeled according to previous reports.[28,29] It was found that the introduction of 0–5 wt% **PFPN** showed negligible influence. This result suggested **PFPN** did not participate in the solvation shell of Li^+ greatly, which should be an important reason for the excellent compatibility of **PFPN**-containing electrolyte. Raman spectra (Fig. 6c and d) also showed similar observation, where the coordination states of EC and DMC were only slightly changed.[30,31] Additionally, the NMR tests were also conducted, and some subtle changes were found. As is shown in Fig. 6e and f, adding **PFPN** led to increasing downfield shift for ^{7}Li NMR and ^{13}C NMR spectra. Nevertheless, these small changes also

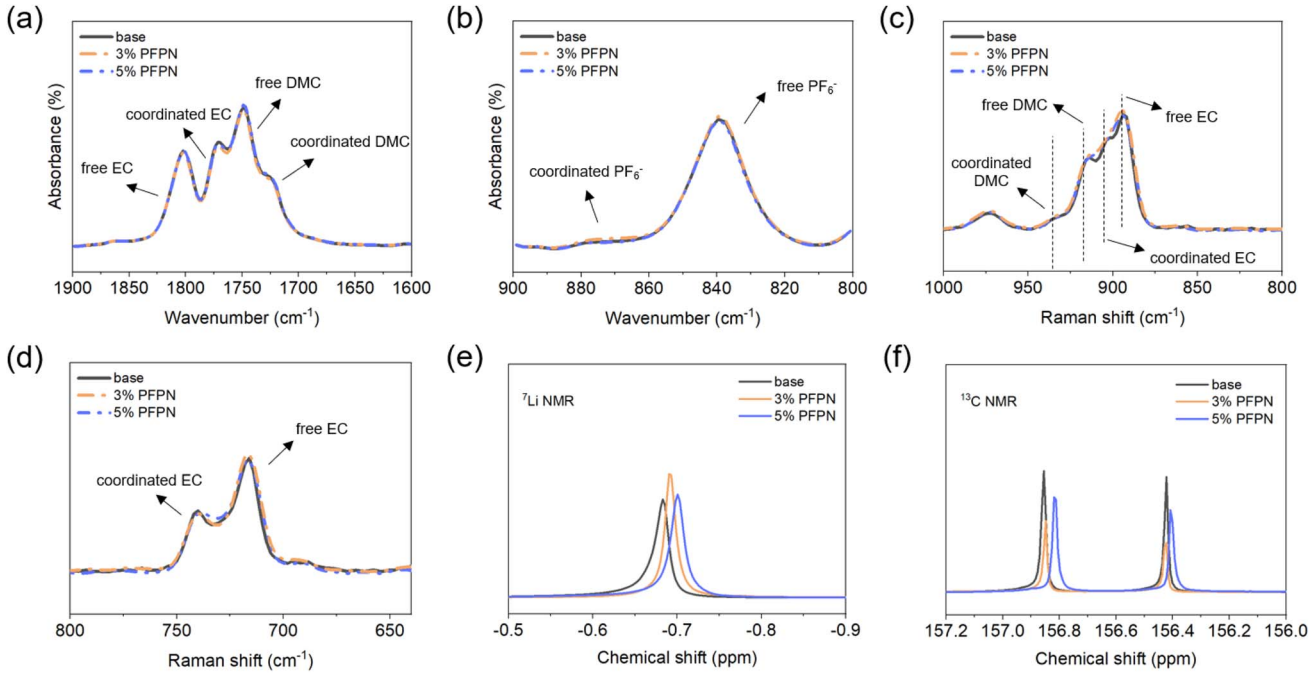

Fig. 6 Solvation structure characterizations of base and **PFPN**-containing electrolytes (a and b) FT-IR spectra, (c and d) Raman spectra and (e and f) NMR spectra.

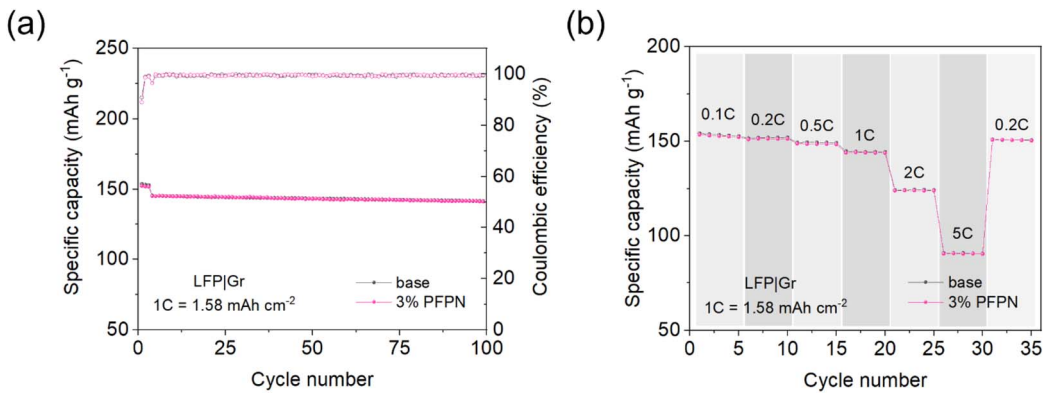

Fig. 7 Electrochemical performance of LFP|Gr cells with different electrolytes: (a) long-term cycling and (b) rate performance.

confirmed that **PFPN** did not present a profound impact on the solvation structure of electrolyte.

To examine the influence of **PFPN**-containing electrolyte on full cells, LFP|Gr full cells were assembled for electrochemical performance test. As is shown in Fig. 7a, the cell with 3% **PFPN** electrolyte showed comparable cycling performance to that with base electrolyte, and the discharge capacity retention rates after 100 cycles were 97.34% for base electrolyte and 97.25% for 3% **PFPN** electrolyte, which once again demonstrated the great electrolyte–electrode compatibility. Additionally, the rate performance was also studied to ensure the application in various scenarios, and it was surprising to find that 3% **PFPN** electrolyte exhibited similar performance even at 5C current density. Combined with the previous SEM and XPS analysis, we believe the desirable rate performance should be attributed to the formation of N-containing SEI species.

4. Conclusion

In summary, **PFPN** was proposed as a flame-retarding additive for Li ion battery electrolyte, and the flammability of electrolyte was greatly suppressed with only 3 wt% content. The compatibility of 3% **PFPN** electrolyte was studied in LFP|Li and Gr|Li half cells, both exhibited comparable performance to base electrolyte. SEM and XPS revealed **PFPN** could form stable electrode/electrolyte interphase, thus prevent continuous parasitic reactions, and the formation of N-containing SEI species was found to be beneficial for Gr anode. FT-IR, Raman and NMR spectra demonstrated **PFPN** did not present great influence on the solvation structure of electrolyte. Benefiting from the excellent compatibility of **PFPN**, LFP|Gr cell presented desirable long-term stability and rate performance, which demonstrates great potential for practical application

and provides a guideline for designing compatible non-flammable electrolyte.

Conflicts of interest

The author declares no conflict of interest.

Acknowledgements

We gratefully acknowledge the financial support from the Science and Technology Project of State Grid Corporation of China under Grant 5108-202218280A-2-76-XG.

References

1 T. Tsujikawa, K. Yabuta, T. Matsushita, T. Matsushima, K. Hayashi and M. Arakawa, Characteristics of lithium-ion battery with non-flammable electrolyte, *J. Power Sources*, 2009, **189**(1), 429–434, DOI: 10.1016/j.jpowsour.2009.02.010.

2 A. Yusuf, V. Sai Avvaru, J. De la Vega, M. Zhang, J. Garcia Molleja and D.-Y. Wang, Unveiling the structure, chemistry, and formation mechanism of an in-situ phosphazene flame retardant-derived interphase layer in $LiFePO_4$ cathode, *Chem. Eng. J.*, 2023, **455**, 140678, DOI: 10.1016/j.cej.2022.140678.

3 H. Q. Pham, H.-Y. Lee, E.-H. Hwang, Y.-G. Kwon and S.-W. Song, Non-flammable organic liquid electrolyte for high-safety and high-energy density li-ion batteries, *J. Power Sources*, 2018, **404**, 13–19, DOI: 10.1016/j.jpowsour.2018.09.075.

4 G. Jiang, J. Liu, Z. Wang and J. Ma, Stable non-flammable phosphate electrolyte for lithium metal batteries *via* solvation regulation by the additive, *Adv. Funct. Mater.*, 2023, **33**(30), 2300629, DOI: 10.1002/adfm.202300629.

5 K. Chatterjee, A. D. Pathak, A. Lakma, C. S. Sharma, K. K. Sahu and A. K. Singh, Synthesis, characterization and application of a non-flammable dicationic ionic liquid in lithium-ion battery as electrolyte additive, *Sci. Rep.*, 2020, **10**(1), 9606, DOI: 10.1038/s41598-020-66341-x.

6 G. Liu, Z. Cao, L. Zhou, J. Zhang, Q. Sun, J.-Y. Hwang, L. Cavallo, L. Wang, Y.-K. Sun and J. Ming, Additives engineered nonflammable electrolyte for safer potassium ion batteries, *Adv. Funct. Mater.*, 2020, **30**(43), 2001934, DOI: 10.1002/adfm.202001934.

7 H. Ota, A. Kominato, W.-J. Chun, E. Yasukawa and S. Kasuya, Effect of cyclic phosphate additive in non-flammable electrolyte, *J. Power Sources*, 2003, **119–121**, 393–398, DOI: 10.1016/S0378-7753(03)00259-3.

8 K. Matsumoto, K. Nakahara, K. Inoue, S. Iwasa, K. Nakano, S. Kaneko, H. Ishikawa, K. Utsugi and R. Yuge, Performance improvement of li ion battery with non-flammable **TMP** mixed electrolyte by optimization of lithium salt concentration and SEI preformation technique on graphite anode, *J. Electrochem. Soc.*, 2014, **161**(5), A831, DOI: 10.1149/2.091405jes.

9 A. Bouibes, S. Saha and M. Nagaoka, Theoretically predicting the feasibility of highly-fluorinated ethers as promising diluents for non-flammable concentrated electrolytes, *Sci. Rep.*, 2020, **10**(1), 21966, DOI: 10.1038/s41598-020-79038-y.

10 W. Wang, C. Liao, L. Liu, W. Cai, Y. Yuan, Y. Hou, W. Guo, X. Zhou, S. Qiu, L. Song, Y. Kan and Y. Hu, Comparable investigation of tervalent and pentavalent phosphorus based flame retardants on improving the safety and capacity of lithium-ion batteries, *J. Power Sources*, 2019, **420**, 143–151, DOI: 10.1016/j.jpowsour.2019.02.037.

11 T. Doi, R. J. Taccori, R. Fujii, T. Nagashima, T. Endo, Y. Kimura and M. Inaba, Non-flammable and highly concentrated carbonate ester-free electrolyte solutions for 5 v-class positive electrodes in lithium-ion batteries, *ChemSusChem*, 2021, **14**(11), 2445–2451, DOI: 10.1002/cssc.202100523.

12 X. L. Yao, S. Xie, C. H. Chen, Q. S. Wang, J. H. Sun, Y. L. Li and S. X. Lu, Comparative study of trimethyl phosphite and trimethyl phosphate as electrolyte additives in lithium ion batteries, *J. Power Sources*, 2005, **144**(1), 170–175, DOI: 10.1016/j.jpowsour.2004.11.042.

13 B. Wu, F. Pei, Y. Wu, R. Mao, X. Ai, H. Yang and Y. Cao, An electrochemically compatible and flame-retardant electrolyte additive for safe lithium ion batteries, *J. Power Sources*, 2013, **227**, 106–110, DOI: 10.1016/j.jpowsour.2012.11.018.

14 J. Feng, X. Gao, L. Ci and S. Xiong, A novel bifunctional additive for 5 v-class, high-voltage lithium ion batteries, *RSC Adv.*, 2016, **6**(9), 7224–7228, DOI: 10.1039/C5RA22547G.

15 H. Cheng, Z. Ma, P. Kumar, H. Liang, Z. Cao, H. Xie, L. Cavallo, Q. Li and J. Ming, Non-flammable electrolyte mediated by solvation chemistry toward high-voltage lithium-ion batteries, *ACS Energy Lett.*, 2024, 1604–1616, DOI: 10.1021/acsenergylett.3c02789.

16 Y. Zou, G. Liu, Y. Wang, Q. Li, Z. Ma, D. Yin, Y. Liang, Z. Cao, L. Cavallo, H. Kim, L. Wang, H. N. Alshareef, Y.-K. Sun and J. Ming, Intermolecular interactions mediated nonflammable electrolyte for high-voltage lithium metal batteries in wide temperature, *Adv. Energy Mater.*, 2023, **13**(19), 2300443, DOI: 10.1002/aenm.202300443.

17 Q. Sun, Z. Cao, Z. Ma, J. Zhang, W. Wahyudi, G. Liu, H. Cheng, T. Cai, E. Xie, L. Cavallo, Q. Li and J. Ming, Interfacial and interphasial chemistry of electrolyte components to invoke high-performance antimony anodes and non-flammable lithium-ion batteries, *Adv. Funct. Mater.*, 2023, **33**(1), 2210292, DOI: 10.1002/adfm.202210292.

18 Y. Zou, Z. Ma, G. Liu, Q. Li, D. Yin, X. Shi, Z. Cao, Z. Tian, H. Kim, Y. Guo, C. Sun, L. Cavallo, L. Wang, H. N. Alshareef, Y.-K. Sun and J. Ming, Non-flammable electrolyte enables high-voltage and wide-temperature lithium-ion batteries with fast charging, *Angew. Chem., Int. Ed.*, 2023, **62**(8), e202216189, DOI: 10.1002/anie.202216189.

19 Y. Li, Y. An, Y. Tian, C. Wei, S. Xiong and J. Feng, High-safety and high-voltage lithium metal batteries enabled by a nonflammable ether-based electrolyte with phosphazene as a cosolvent, *ACS Appl. Mater. Interfaces*, 2021, **13**(8), 10141–10148, DOI: 10.1021/acsami.1c00661.

20 H. Fei, Y. An, J. Feng, L. Ci and S. Xiong, Enhancing the safety and electrochemical performance of ether based

lithium sulfur batteries by introducing an efficient flame retarding additive, *RSC Adv.*, 2016, **6**(58), 53560–53565, DOI: **10.1039/C6RA08552K**.

21 S. Zhang, S. Li and Y. Lu, Designing safer lithium-based batteries with nonflammable electrolytes: a review, *eScience*, 2021, **1**(2), 163–177, DOI: **10.1016/j.esci.2021.12.003**.

22 Y.-Z. Quan, Q.-S. Liu, M.-C. Liu, G.-R. Zhu, G. Wu, X.-L. Wang and Y.-Z. Wang, Flame-retardant oligomeric electrolyte additive for self-extinguishing and highly-stable lithium-ion batteries: beyond small molecules, *J. Energy Chem.*, 2023, **84**, 374–384, DOI: **10.1016/j.jechem.2023.05.041**.

23 B. Li, Y. Wang, H. Rong, Y. Wang, J. Liu, L. Xing, M. Xu and W. Li, A novel electrolyte with the ability to form a solid electrolyte interface on the anode and cathode of a $LiMn_2O_4$/graphite battery, *J. Mater. Chem. A*, 2013, **1**(41), 12954–12961, DOI: **10.1039/C3TA13067C**.

24 Y. Qian, P. Niehoff, M. Börner, M. Grützke, X. Mönnighoff, P. Behrends, S. Nowak, M. Winter and F. M. Schappacher, Influence of electrolyte additives on the cathode electrolyte interphase (CEI) formation on $LiNi_1/3Mn1/3Co1/3O_2$ in half cells with Li metal counter electrode, *J. Power Sources*, 2016, **329**, 31–40, DOI: **10.1016/j.jpowsour.2016.08.023**.

25 X. Li, W. Li, L. Chen, Y. Lu, Y. Su, L. Bao, J. Wang, R. Chen, S. Chen and F. Wu, Ethoxy (pentafluoro) cyclotriphosphazene (**PFPN**) as a multi-functional flame retardant electrolyte additive for lithium-ion batteries, *J. Power Sources*, 2018, **378**, 707–716, DOI: **10.1016/j.jpowsour.2017.12.085**.

26 Q. Zhang, L. Xu, X. Yue, J. Liu, X. Wang, X. He, Z. Shi, S. Niu, W. Gao, C. Cheng and Z. Liang, Catalytic current collector design to accelerate $LiNO_3$ decomposition for high-performing lithium metal batteries, *Adv. Energy Mater.*, 2023, **13**(43), 2302620, DOI: **10.1002/aenm.202302620**.

27 S. Kim, K.-Y. Cho, J. Kwon, K. Sim, D. Seok, H. Tak, J. Jo and K. Eom, An inorganic-rich sei layer by the catalyzed reduction of $LiNO_3$ enabled by surface-abundant hydrogen bonding for stable lithium metal batteries, *Small*, 2023, **19**(26), 2207222, DOI: **10.1002/smll.202207222**.

28 D. M. Seo, S. Reininger, M. Kutcher, K. Redmond, W. B. Euler and B. L. Lucht, Role of mixed solvation and ion pairing in the solution structure of lithium ion battery electrolytes, *J. Phys. Chem. C*, 2015, **119**(25), 14038–14046, DOI: **10.1021/acs.jpcc.5b03694**.

29 S. Bertilsson, F. Larsson, M. Furlani, I. Albinsson and B.-E. Mellander, Lithium-ion battery electrolyte emissions analyzed by coupled thermogravimetric/fourier-transform infrared spectroscopy, *J. Power Sources*, 2017, **365**, 446–455, DOI: **10.1016/j.jpowsour.2017.08.082**.

30 M. Morita, Y. Asai, N. Yoshimoto and M. Ishikawa, A Raman spectroscopic study of organic electrolyte solutions based on binary solvent systems of ethylene carbonate with low viscosity solvents which dissolve different lithium salts, *J. Chem. Soc. Faraday Trans.*, 1998, **94**(23), 3451–3456, DOI: **10.1039/A806278A**.

31 S. Uchida and T. Kiyobayashi, How does the solvent composition influence the transport properties of electrolyte solutions? $LiPF_6$ and LiFSA in EC and DMC binary solvent, *Phys. Chem. Chem. Phys.*, 2021, **23**(18), 10875–10887, DOI: **10.1039/D1CP00967B**.